AN ASYNCHRONOUS PULSE-AMPLITUDE PULSE-WIDTH MODEL OF THE HUMAN OPERATOR

by

M. J. Merritt and G. A. Bekey

This research was sponsored by the National Aeronautics and Space Administration under Grant No. NGR 05-018-022.

This paper was prepared for presentation at the USC-NASA Conference on Manual Control, March 1, 2 and 3, 1967 in Los Angeles, California.

AN ASYNCHRONOUS PULSE-AMPLITUDE PULSE-WIDTH MODEL OF THE HUMAN OPERATOR

M. J. Merritt and G. A. Bekey

INTRODUCTION

In order to develop a model for the behavior of a human operator performing a manual control task it is necessary to make some assumptions concerning the operator's inputs and outputs. If it is assumed that the operator utilizes the input continuously and produces continuous outputs then there are a wide variety of techniques which can be used to develop complete human operator models. These techniques include spectral analysis (7, 11), multiple linear regression (13), and gradient search model identification (8). Another assumption which has been studied is that the human operator samples the inputs periodically and produces continuous outputs. The physiology of the optical, neuro-muscular, and cerebral systems (9) supports this assumption. Sampling human operator models are difficult to identify due to the interactions between the sampling rate and time constants in the continuous portion of the model. For simple controlled elements (1, 2) and step inputs (5) complete human operator models have been identified.

Although the physiology supports the use of sampled data models for human operators, many studies have produced no evidence of periodic sampling behavior. In a recent study (7) the power spectrum of the model remnant was examined for periodicities corresponding to sampling phenomena. No evidence of periodic sampling was found. However, experi-

ments conducted at the University of Southern California have shown that small random perturbations about a nominal sampling interval tend to mask periodicities in the spectrum of the model remnant. The sampling behavior of human operators is certainly aperiodic and possibly controlled by a supervisory input monitor. This results in aperiodic input dependent sampling, which may also contain random variations in the sampling interval. If this is indeed the case, the model remnant would not contain strong periodicities.

When the dynamics of the controlled element contain two or more integrations the performance of the human operator approaches that of a bang-bang system. In particular, the double integrator plant, $1/s^2$, usually elicits pulse responses from human operators (4, 6, 14). A mathematical model to represent this output behavior could contain sampled inputs with continuous supervisory control of the sampling. This supervised sampling extends the periodic sampling of previous models (1, 2) to aperiodic input-dependent sampling. The pulse nature of the output makes it possible to relate pulse events to decision surfaces in the error phase space (9, 15).

The object of this paper is to describe the development of a human operator model which produces discrete outputs in response to continuously presented gaussian random inputs. Computer procedures for the complete identification of all model parameters are described.

I. STATEMENT OF THE PROBLEM

A block diagram of the compensatory tracking situation used in this study is shown in Figure 1, and a portion of a typical tracking record is found in Figure 3. An examination of the human operator output (stick position) reveals a sequence of pulses which are roughly triangular in shape. For the purposes of this study, the actual human operator output was converted to the idealized human operator output, as seen in Figure 3. The selection of symmetric triangular pulses as ideal human operator pulses is arbitrary, and other pulse shapes can be used. Further it was decided to treat each pulse as a seperate event, uncorrelated with previous pulses, in order to keep the structure of the pulse model as simple as possible. The use of pre-programmed pulse sequences (3, 10, 12) presents an opportunity for future extensions of the work.

The idealized human operator output can be represented by a sequence of three-tuples: time of the pulse initiation, pulse amplitude, and pulse width. If a causal relationship exists between the transient human operator inputs and the pulse outputs, then the input record can be reduced to samples of the input in the vicinity of the pulse initiation. The objective of the present study is the determination of the relationships between these input samples and the pulse output.

Since each event is treated independently, short term human operator variations are easily computed. These variations are the difference between the model outputs and the actual human operator outputs. The distribution functions of these variations can be obtained and, if desired, can be re-

inserted as model perturbations to produce a human operator model statistically indistinguishable from the actual human operator. The distribution functions and their associated parameters (mean and moments) can be used as measures of performance and state of training.

II THE EXPERIMENT

The compensatory tracking task shown in Figure 1 was mechanized using a Beckman 2132 analog computer, an X-Y oscilloscope and side arm control stick. Operator distraction was minimized by placing the manual control station inside a sound proof enclosure with approximately 40 db of audio attentuation. The operator wore an aircraft type headset with lip microphone for communication purposes. The operator sat in a chair without armrests facing the display oscilloscope. The control stick was adjustable in position and contained an integral arm rest. The operator adjusted the control stick and arm rest into a comfortable position. The oscilloscope was placed at eye level.

The double integrator plant closely resembles an aircraft pitch axis. The input is elevator position and the output is altitude. In order to preserve this resemblance, the error display was a rotating needle corresponding to a glide path indicator in an aircraft navigational /ILS display. Horizontal needle position represented zero error. The frequency response problems associated with actual instruments were avoided by simulating the glide slope needle with an oscilloscope containing a specially prepared edge-lighted reticle.

The control stick and oscilloscope were connected to the analog computer which converted the stick output to a voltage, computed the plant response, and generated the necessary X and Y axis signals for the error display. By solving some of the equations explicitly it was possible to obtain the error and its exact derivative. The inputs to the system were obtained by filtering the output of a low frequency gaussian noise source. The filter transfer function was:

$$F(s) = \frac{K}{(10s + 1)\,(s+1)^3} \tag{1}$$

An FM magnetic tape recorder was used to record tracking data, which was later digitized and stored on a disk file for digital processing.

A single subject received approximately 20 hours of training over a period of one month. The training sessions consisted of 10 minutes of tracking with 10 minute rest periods. One of the last sessions was recorded on magnetic tape. From the 10 minute session approximately 3 minutes of data was subsequently digitized. The sampling interval utilized was 25 milliseconds or 40 samples per second.

The digitized data stored on the 1311 disk file was printed out and punched on IBM cards for permanent storage. The following data was punched on IBM cards:

1. The time of the pulse initiation.
2. The time of the pulse termination.
3. The peak amplitude of the pulse.

4. The values of e and $\dot{e}$ at the following times:

   a. One sample after the initiation of the pulse.

   b. At the start of the pulse.

   c. The 5 samples prior to the start of the pulse.

III HUMAN OPERATOR MODEL

In order to carry out modeling efforts, a basic model structure must be hypothesized. Intuitive concepts of human operator behavior and an examination of the tracking record, Figure 3, led to the model shown in Figure 2. This model is based on the assumption that the operator generates an output consisting of a series of modulated pulses. The width and amplitude of these pulses are dependent on the error and error rate at some time prior to pulse initiation. Consequently, the next phase of the modeling effort consisted of investigating possible quantitative relationships between the input quantities (error and error rate) and the output pulse events.

A. Pulse amplitude relationships

The amount of pulse amplitude modulation utilized by the human operator is evidenced in the distribution function of the pulse amplitudes, Figure 4. Evidently the operator does not behave in a bang-bang mode. In fact, he utilizes a width range of amplitudes. Further work is needed to evaluate the significance of the asymmetry which appears in the data. Consider the idealized triangular pulse output record shown in Figure 3. The relationship between the inputs and the pulse amplitude was

postulated to be:

$$c_1\, e(t_i - \tau_1) + c_2\, \dot{e}\,(t_i - \tau_1) + c_3 = p_i \tag{2}$$

where c_1, c_2, and c_3 are constants, τ_1 is the time delay, shown in Figure 2, t_i are the times of pulse initiation, as shown in Figure 3., and e and $\dot{e}$ are the human operator inputs.

The constants c_1, c_2 and c_3 are easily determined for fixed values of τ_1. This procedure is natural since the digitizing of the tracking record with a sampling interval of T = 25 milliseconds allows τ_1 to take on only discrete values which are multiples of T. Let τ_1^* be one of these fixed values of τ_1. If there are N events (human operator pulses) then there are N equations in three unknowns:

$$\begin{aligned} p_1 &= c_1\, e(t_1 - \tau_1^*) + c_2\, \dot{e}\, (t_1 - \tau_1^*) + c_3 \\ p_2 &= c_1\, e(t_2 - \tau_1^*) + c_2\, \dot{e}\, (t_2 - \tau_1^*) + c_3 \\ &\vdots \\ p_N &= c_1\, e(t_N - \tau_1^*) + c_2\, \dot{e}\, (t_N - \tau_1^*) + c_3 \end{aligned} \tag{3}$$

or, in vector form

$$p = Ac \tag{4}$$

where A is an N X 3 matrix of the values of e and $\dot{e}$. A least squares error criterion is:

$$\phi = (p - Ac)'\,(p - Ac) \tag{5}$$

which is a positive definite quadratic function of the parameter vector, c. In expanded form.

$$\emptyset = p'p - 2c'A'p + c'A'Ac \tag{6}$$

The gradient of the criterion function is:

$$\nabla_c \emptyset = -2A'p + 2A'Ac \tag{7}$$

A stationary point of the criterion function is found by setting

$$\nabla_c \emptyset = 0 \tag{8}$$

which yields

$$A'Ac = A'p \tag{9}$$

Finally

$$c = [A'A]^{-1} A'p \tag{10}$$

The parameter vector, c, which results from this computation represents those values of c_1, c_2 and c_3 which produce the best least squares fit between the pulse amplitude predicted by the model

$$PM_i = c_1 e(t_i - \tau_1^*) + c_2 \dot{e}(t_i - \tau_1^*) + c_3 \tag{11}$$

and the pulse amplitudes (p_i) for a given value of τ_1, say τ_1^* and $i = 1, 2, \ldots N$.

The criterion function, $\emptyset$, is a measure of the correlation between the model relationship and the experimental data. In order to gain more insight into the problem, the values of PM_i may be plotted against the actual pulse amplitude p_i for each of the N pulse events. If the human operator were invariant with time and the model an exact representation,

the plotted points would lie on a straight line with a slope of one, corresponding to a criterion function of zero. There are two ways in which the optimal value for τ_1 can be selected from the set of values τ_1^* used in the linear regression routine above. The first is to examine the point plots just described for various values of τ_1^* selecting the plot which produced the best visual approximation to a perfect straight line. The second method is to select that value of τ_1^* which produces the minimum criterion function, $\emptyset$. Both methods will be used below in analyzing and interpreting the results from the least squares linear regression analysis.

B. Computer Results

A least squares linear regression routine mechanizing the procedure described above was written. In order to make possible the investigation of asymmetry in the human operator's response, the positive and negative pulses of the tracking record were analyzed separately. The results of these computations are tabulated in Table 3 and plotted in Figures 5 and 6.

TABLE 3

τ_1^*	c_1		c_2		c_3		$\emptyset \times 10^{-6}$	
Polarity	+	-	+	-	+	-	+	-
0.125	-0.060	-0 065	-0.139	-0.145	2.16	-2.02	0.507	0.220
0 100	-0.061	-0.066	-0.134	-0.143	2.16	-1.99	0.496	0.217
0.075	-0.062	-0.065	-0.130	-0.137	2.16	-2.00	0.495	0.222
0.050	-0.062	-0.064	-0.125	-0.131	2.16	-2.04	0.492	0.228
0.025	-0.059	-0.061	-0.118	-0.123	2.19	-2.10	0.498	0.242
0	-0.057	-0.060	-0.112	-0.116	2.22	-2.14	0.504	0.253
-0.025	-0.057	-0.060	-0.106	-0.108	2.25	-2.20	0.509	0.263

A plot of the criterion function, $\emptyset$, versus τ_1^* is found in Figure 6. From this figure it can be seen that the minimums are well defined. The scatter plot of model pulse amplitude PM_i versus the actual pulse amplitude p_i is found in Figure 5. The groupings are quite close to the ideal unity slope line. The optimum values for positive and negative pulses, respectively are c_1 = -0.062, -0.066; c_2 = -0.125, -0.143; c_3 = 2.16, -1.99; and τ_1 = 0.050, 0.100. The symmetry observed in these values contrasts with the large differences in optimum criterion function, $\emptyset_+$ = .492 and $\emptyset_-$ = 0.217. In other words, the positive pulses produced poorer correlation than the negative pulses. This may be a result of one or more of the following factors: arm motion asymmetry associated with the side arm control stick, incomplete training, or the tendency of the operator to prefer certain portions of the error phase plane (also a well-known result of incomplete training).

An analysis of the differences between human operator amplitude and the corresponding model pulse amplitude serves two purposes. The accuracy of the model may be measured and the distribution function of the human operator variations may be determined. The mean and standard deviation of these functions are:

TABLE 4

	Pulse Polarity	
	+	-
Mean (volts)	0	0
Standard Deviation (volts)	0.80	0.58

The amplitudes of human operator pulses range from 0.5 to 6.0 volts, with a distribution function as shown in Figure 4. One standard deviation represents about 40% error. Alternatively, noise of the same mean and standard deviation or the same distribution function could be added to the pulse amplitude model output.

C. Pulse Width Relationships

Preliminary analysis of the tracking records led to the hypothesis that the pulse width was proportional to the pulse amplitude. The results below indicate that this is not necessarily the best model structure. A future study might consider the pulse width as another degree of freedom which is determined independently of pulse amplitude. A plot of pulse width versus pulse amplitude for each of the 150 events is found in Figure 7. The pulse width appears to be independent of pulse amplitude. Least squares linear regression was used to determine the optimal parameter values in the following equation:

$$c_1 p_i + c_2 = pw_i \tag{12}$$

The positive and negative pulses were treated separately. The optimal parameter values are $c_1 = -0.0205, -0.0492$ and $c_2 = 0.7110, 0.3157$. The differences between the human operator and the model outputs were computed. The mean and standard deviation of these differences are:

TABLE 5

	Pulse Polarity	
	+	-
Mean (sec.)	0	0
Standard Deviation (sec.)	0.05	0.04

The values of pw_i range from 0.3 to 0.9 seconds. One standard deviation represents a maximum error of 16%. As with the pulse amplitude model, the output of the pulse width model could be perturbed by random noise possessing the same distribution functions.

D. Pulse Initiation

The results of the pulse amplitude model clearly demonstrate the ability of the human operator to estimate the derivative of displayed signals. The pulse initiation decision model is based on this ability and the intuitive feeling that the human operator utilized a control policy which results in a relatively simple decision surface in the error phase space. Inspection of the error phase plane trajectories immediately preceding pulse initiation led to the observation that the human operator utilizes the favorable error rate in the second and fourth quadrants by allowing the system to coast until the magnitude of the error is sufficiently small. If at that time, the error rate is still large, a new pulse event occurs. A further observation is that an error-error rate dead zone exists inside of which no pulse events are generated. This is consistent with other human operator

tracking experiments [1, 15].

Based on the above observations, it was hypothesized that the initiation of an output pulse by the human operator is a complex process which consists of several phases as follows:

(a) Somewhere near the completion of an output pulse, monitoring of e and $\dot{e}$ by a decision element starts.

(b) When the error trajectory enters pre-selected regions of the phase plane, a decision to produce a pulse is made.

(c) Some time later a pulse is generated.

The treatment of each pulse as an individual event places restrictions on the decision element. A number of investigators [1, 2, 7, 9, 10, 15] have determined human operator reaction times to be between 150 and 300 milliseconds. In Figure 8 is found the distribution function of the times between pulses. There are a large number of pulses spaced less than 200 milliseconds apart. These pulses probably correspond to pre-programmed pulse sequences [3, 12]. The human operator generates single pulses (rate corrections) and pulse sequences (position corrections). A continuation of this study would include a pulse program decision element as described by Bekey and Angel [3]. With this limitation in mind, the identification of the decision element was undertaken.

Inspection of the error phase plane trajectories led to the pulse initiation model shown below in Figure 9.

A criterion function selected in accordance with the verbal description above is

$$\phi(R, \theta) = \frac{1}{150} \sum_{i=1}^{150} \left[\tau_2 - (t_i - t_{im}) \right]^2 \qquad (13)$$

where:

R is the radius of a circular threshold region in the error phase plane (See Fig. 9.)

θ is an angle defined in Figure 9.

t_i is the time of initiation of the i-th pulse

t_{im} is the time at which the region of the error phase plane defined by R and θ in Fig. 9 is entered (i.e., a decision to generate the i-th pulse is made by the model)

τ_2 is the time delay between decision and initiation, as defined by

$$\tau_2 = \frac{1}{150} \sum_{i=1}^{150} (t_i - t_{im}) \qquad (14)$$

The criterion function, eq. (13) is the variance of the delay time.

A systematic study of the R, θ parameter plane was conducted. The optimum parameter values were found to be R = 4.0 volts, $\theta = 35^{\circ}$ and $\tau_2 = 0.200$ sec. The distribution of differences between model pulse initiation and human operator pulse initiation times is found in Figure 10. The peak at 100 milliseconds late is probably due to preprogrammed pulse sequences. The use of more complex decision elements is clearly indicated. However, these results demonstrate the applicability of discrete decision elements to the development of input dependent sampling human operator models.

IV THE COMPLETE HUMAN OPERATOR MODEL

The complete human operator model is shown in Figure 11. The parameters of this model have been identified as described above. The completely identified human operator model for one well trained subject is found in Figure 12.

V SUMMARY OF RESULTS AND CONCLUSIONS

The parameters of the human operator model shown in Figure 11 were identified from experimental data taken from one subject in an advanced state of training. No records were made of the error or measures of the error as a function of training. The computational results brought to light a number of interesting results:

(1) The delay time τ_2 between the model's decision to pulse and actual event was 200 milliseconds. The value is within the range of reaction times reported in the literature [1, 2, 7, 9, 10, 15].

(2) The numerical values for the time delays in Figure 12 lead to the following sequence: (1) A decision is made to generate a pulse, followed by (2) a pause of 100-150 milliseconds, (3) e (t) and $\dot{e}$ (t) we sampled (4) during the next 50-100 milliseconds the amplitude and width of the pulse are computed (5) the pulse is generated.

(3) The pulse amplitude and pulse-width models for negative pulses produce better correlations with the experimental data than the models for positive pulses. This is clearly apparent

in the scatter plot, Figure 5 and in the values of the criterion function $\emptyset$, Figure 6. This may be the result of incomplete training, the design of the side arm controller used, the position of the subject's arm relative to the controller or a characteristic of the particular human operator in this experiment.

(4) The pulse amplitude models for positive and negative pulses are quite similar, despite considerable asymmetry in pulse amplitude distributions, Figure 4.

(5) The results presented in Figure 8 strongly indicate that human operators utilize some pre-programmed pulse sequences.

(6) If the differences between model results and experimental tracking data are viewed as the result of short term human operator variations, then the statistics of the human operator variations are easily determined, [tables 4 and 5].

From the present study it is not feasible to determine whether the model errors observed are random or functionally dependent on the human operator inputs and input-output history. Further studies should include pre-programmed pulse elements, more complex error phase plane decision surfaces, and the effects of training on the model parameters and their associated distribution functions.

REFERENCES

1. Bekey, G. A. "Sampled Data Models of the Human Operator in a Control System", Ph.D. dissertation, University of California at Los Angeles, 1962.

2. Bekey, G. A., "The Human Operator as a Sampled Data System", IRE Transactions, Vol. HFE-3, No. 2, Sept. 1962

3. Bekey, G. A., and Angel, E. S., "Asynchronous Finite State Models of Manual Control Systems", University of Southern California, Electronic Sciences Laboratory Report USCEE-160 1966.

4. Elkind, J. I., Kelley, J. A. , and Payne, R. A., "Adaptive Characteristics of the Human Controller in Systems Having Complex Dynamics", Proceedings of the Fifth National Symposium on Human Factors in Electronics, 1964.

5. Fu, K. S. and Knoop, D. E., "An Adaptive Model of the Human Operator in a Control System", Purdue University Report TREE 64-15, 1964.

6. Kelley, Charles R., "Design Applications of Adaptive (Self Adjusting) Simulators", Proceedings of NASA-MIT Working Conference on Manual Control, February 28-March 2, 1966.

7. McRuer, D. and Graham, D., "Human Pilot Dynamics in Compensatory Systems", Technical Report No. AFFDL-TR-65-15.

8. Meissinger, H. F. and Bekey, G. A., "An Analysis of Continuous Parameter Identification Methods", Simulation, February 1966.

9. Pew, Richard W., "Temporal Organization in Skilled Performance", University of Michigan Technical Report 02814-11-T, 1963

10. Pew, Richard W., "Performance of Human Operators in a Three-State Relay Control System with Velocity-Augmented Displays", IEEE Transactions on Human Factors in Electronics, Vol. 7 No. 2 June, 1966.

11. Todosiev, E. P., Rose, R. E. , Bekey, G. A., and Williams, H. L., "Human Tracking Performance in Uncoupled and Coupled Two Axis Systems", TRW Systems Report 4380-6003-R0000, 1965.

12. Tomovic, R. and McGhee, R. B., "A Finite State Approach to the Synthesis of Bioengineering Systems", IEEE Transactions on Human Factors in Engineering. Vol. 7 No. 2, June 1966.

13. Wierwille, W. W., "A Theory for Optimal Deterministic Characterization of Time Varying Human Operator Dynamics", Cybernetics, Human Factors, IEEE Convention Record, Part 6, 1965.

14. Young, L. R. and Meiry, J. L., "Manual Control of an Unstable System with Visual and Motion Cues", IEEE Convention Record, Part 6, 1965.

15. Young, L. R. and Stark, L. "Biological Control Systems - A Critical Review and Evaluation", NASA Contractor Report CR-190, 1965.

16. Elkind, J. E., et al, "Evaluation of a Technique for Determining Time-Invariant and Time-Variamt Dynamic Characteristics of Human Pilots", NASA Tech Note D-1897, May 1963.

ILLUSTRATIONS

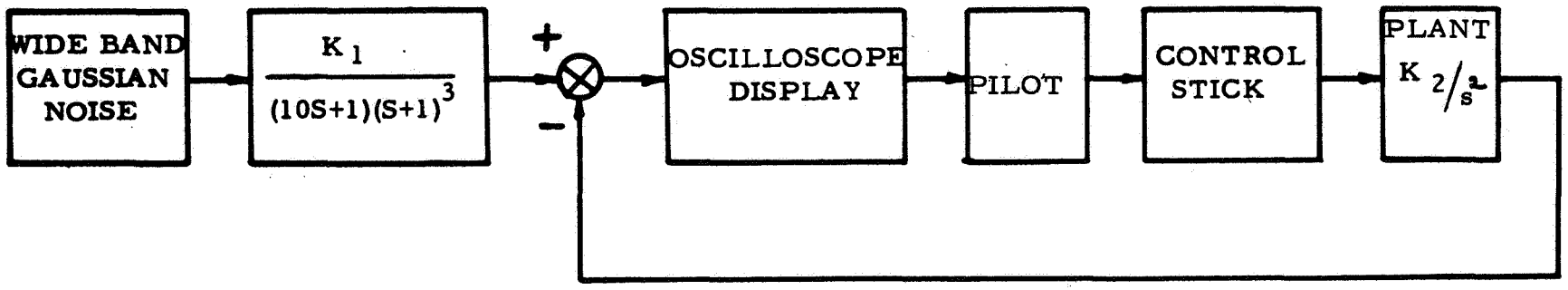

FIGURE 1 - COMPENSATORY TRACKING SYSTEM

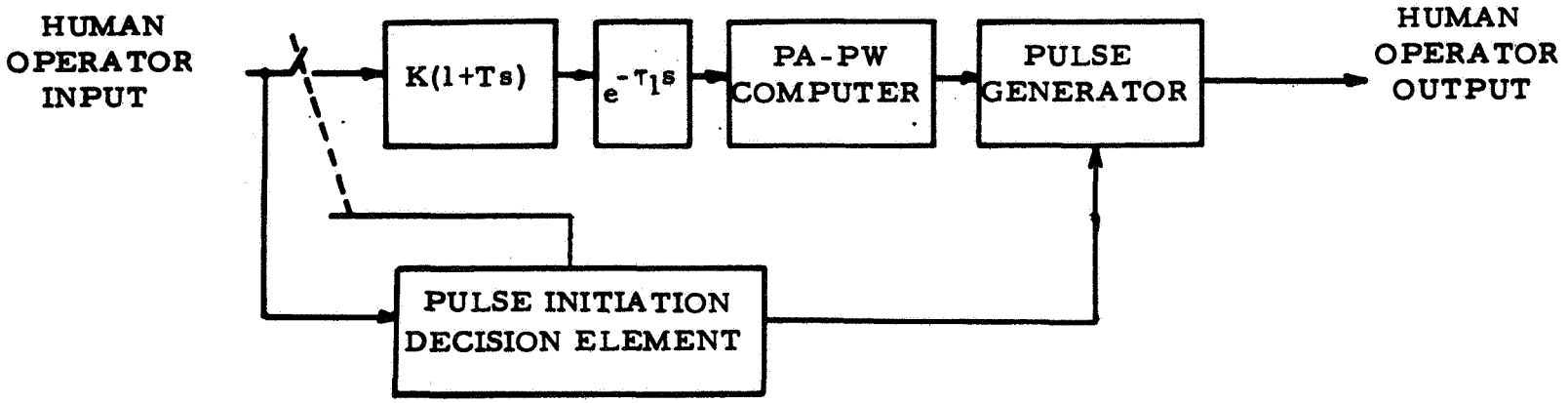

FIGURE 2 - GENERAL FORM OF PROPOSED HUMAN OPERATOR MODEL

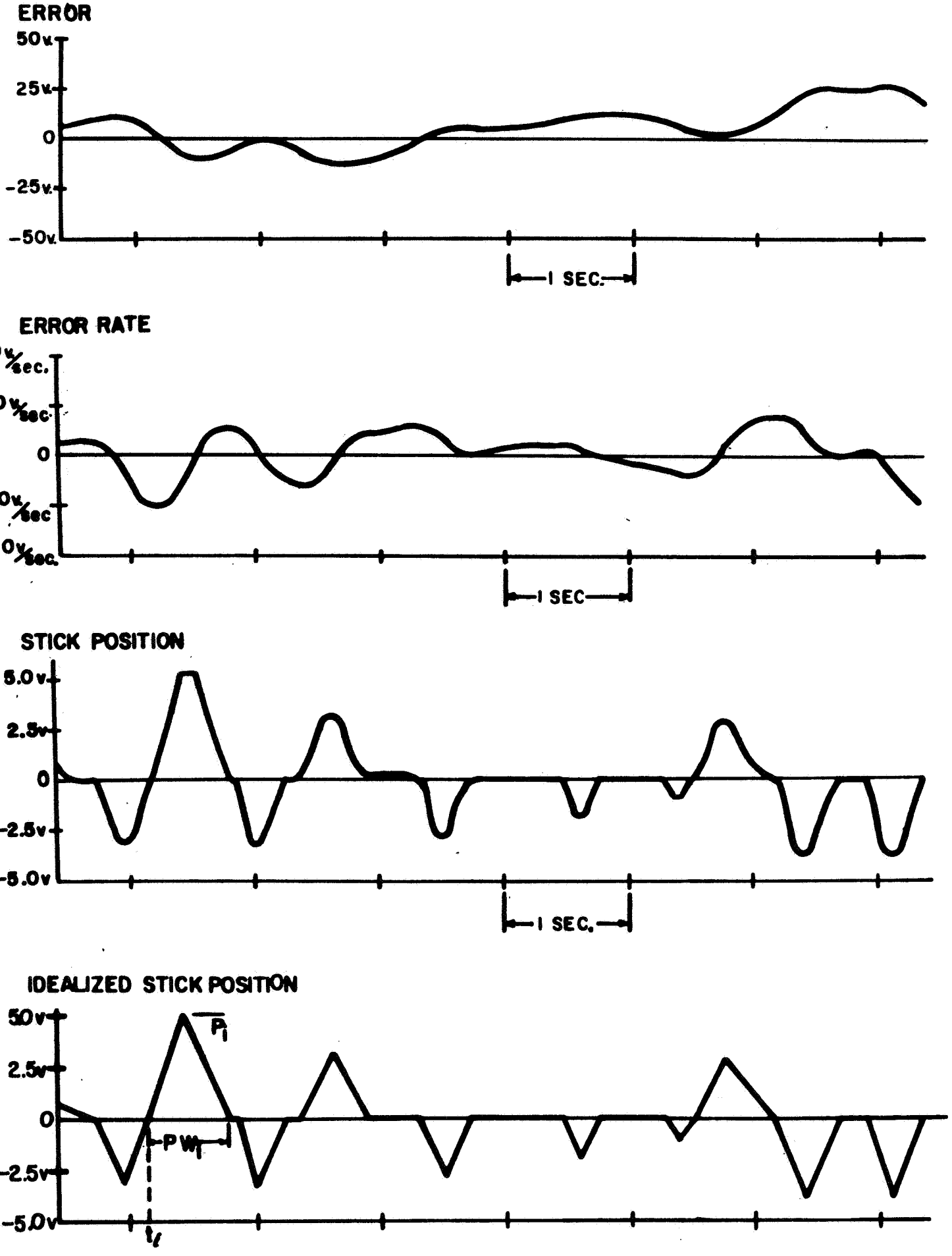

FIGURE 3 TYPICAL TRACKING RECORD

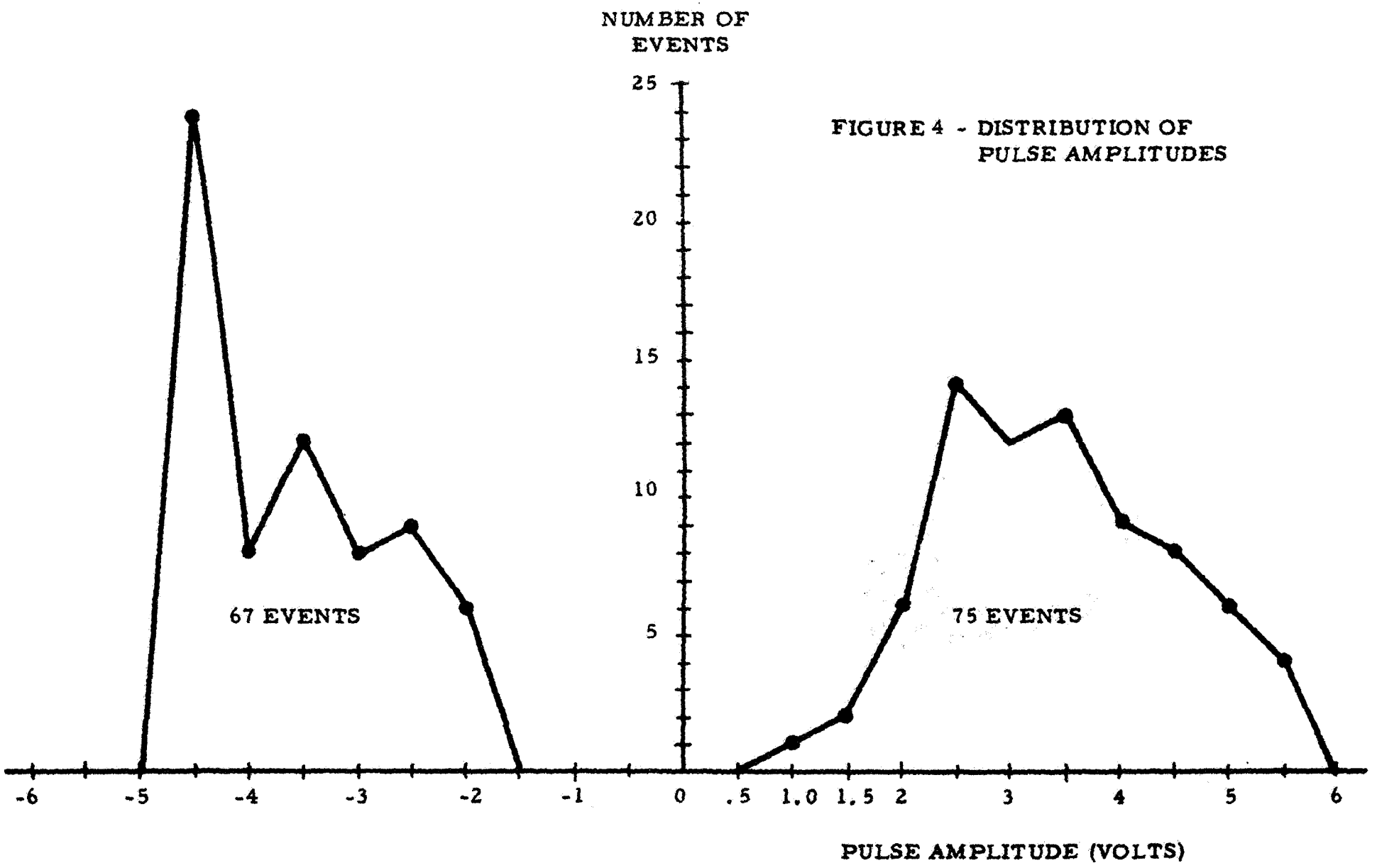

FIGURE 4 - DISTRIBUTION OF PULSE AMPLITUDES

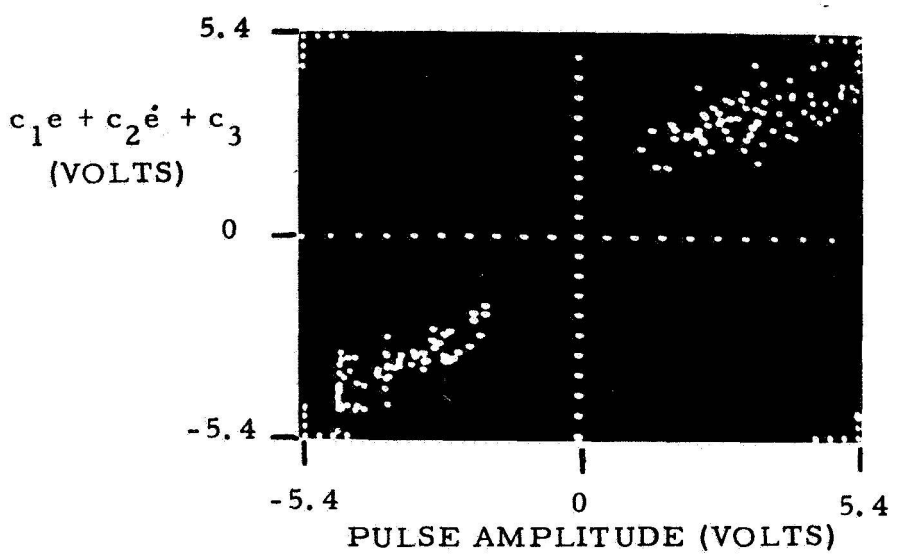

FIGURE 5 - $c_1e + c_2\dot{e} + c_3$ Vs PULSE AMPLITUDE, POSITIVE AND NEGATIVE PULSES OPTIMIZED SEPARATELY

FIGURE 6 - CRITERION FUNCTION FOR PULSE AMPLITUDE MODEL Vs TIME DELAY (τ_1^*)

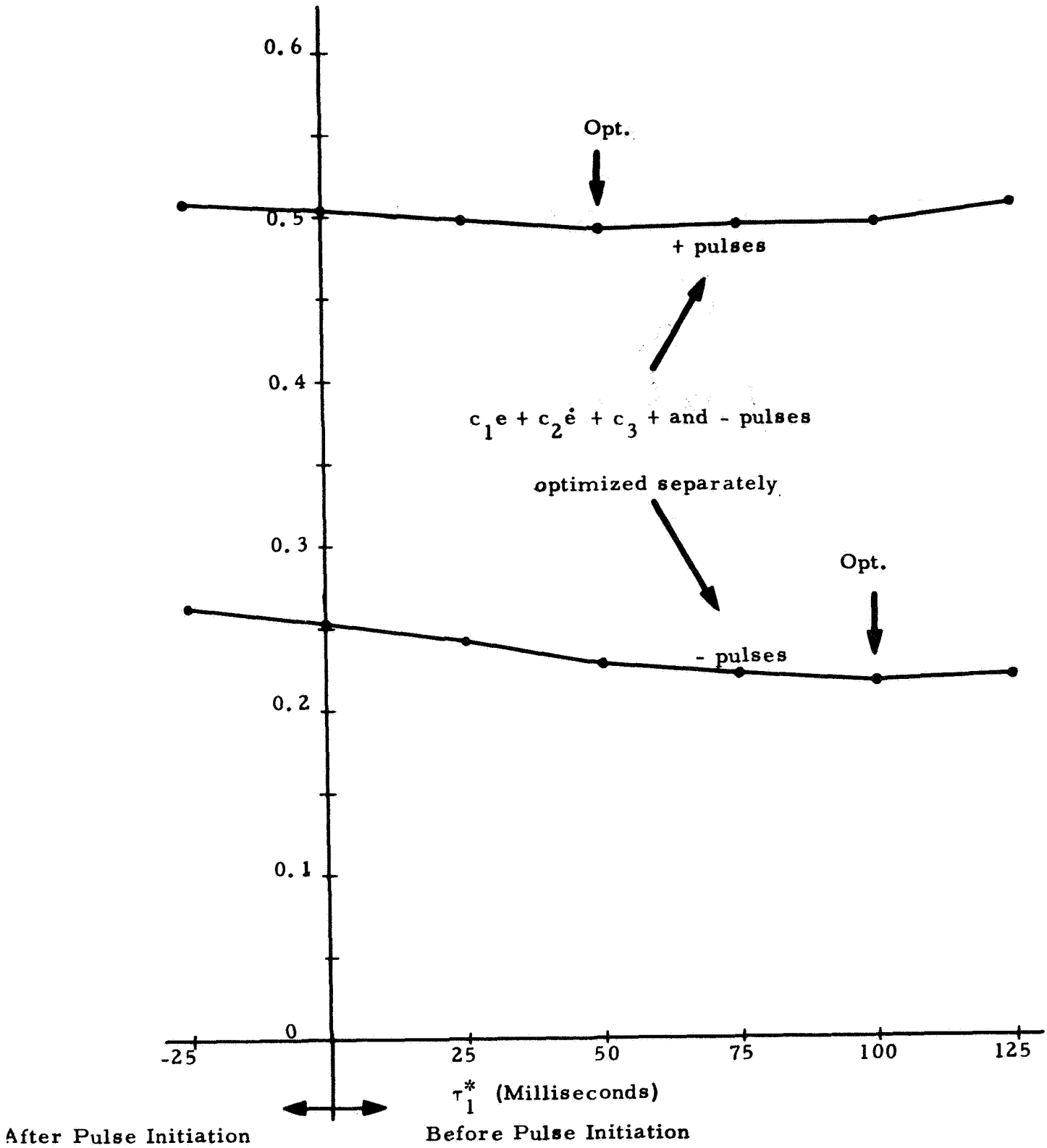

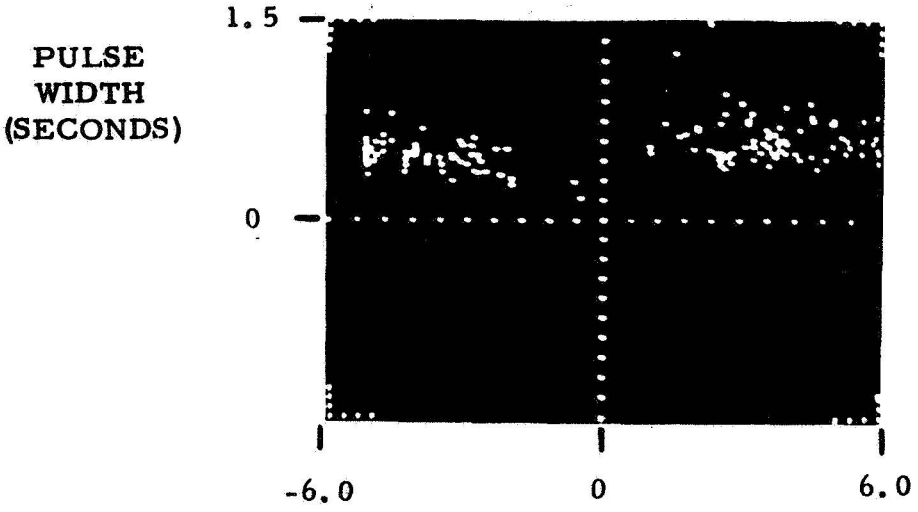

FIGURE 7 - PULSE WIDTH Vs PULSE AMPLITUDE

FIGURE 8 - DISTRIBUTION FUNCTION OF THE MAGNITUDE OF THE TIME INTERVAL BETWEEN PULSE EVENTS (FROM THE TERMINATION OF THE i TH EVENT TO THE START OF THE i + 1ST EVENT)

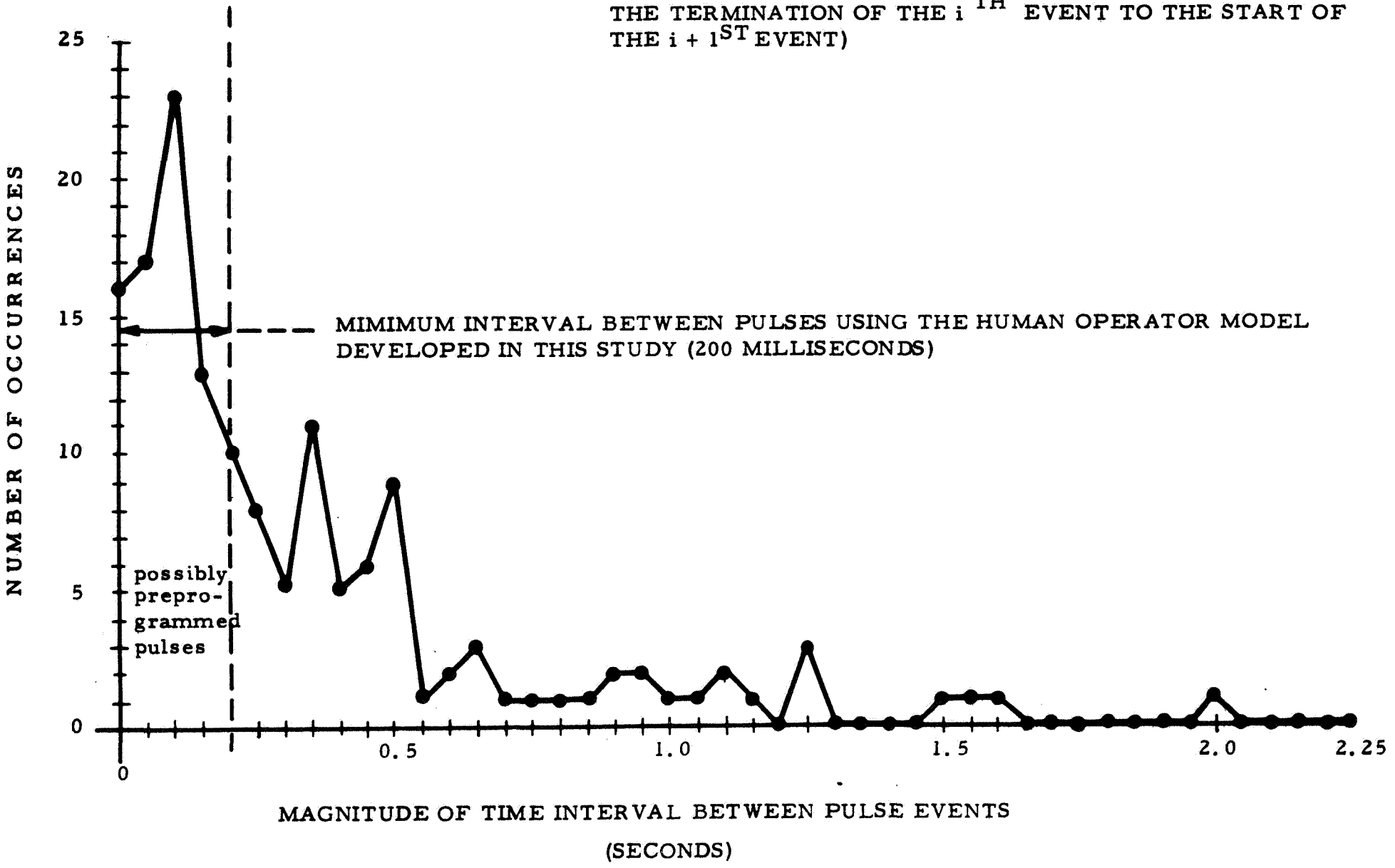

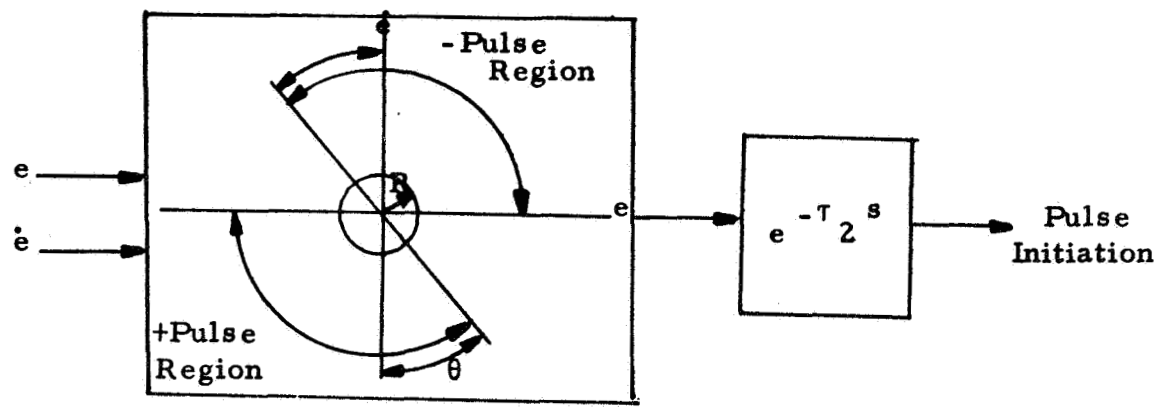

FIGURE 9 - PULSE INITIATION DECISION ELEMENT

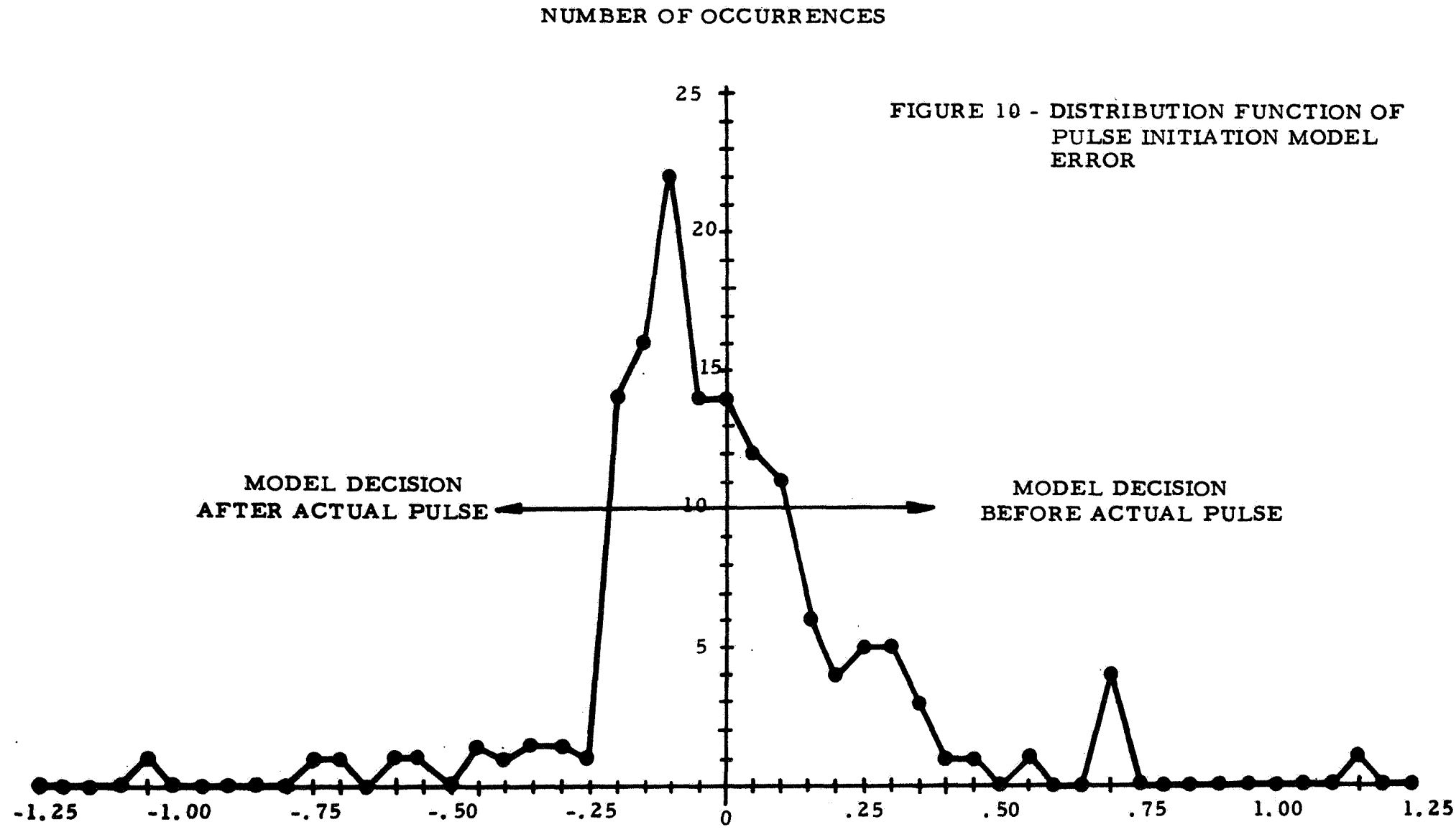

FIGURE 10 - DISTRIBUTION FUNCTION OF PULSE INITIATION MODEL ERROR